Engineering Solutions to Mechanics, Marine Structures and Infrastructures

Eng. Solut. Mech. Mar. Struct. Infrastruct.
2024.1(3).10
ISSN: 3006-2837
https://doi.org/10.58531/esmmsi/1/3/10

Review

A Review of Wind-Induced Swing Response Calculations for Transmission Conductors

Yi Gu, Yuelong Zhang*

China Energy Engineering Group Zhejiang Electric Power Design Institute Co., Ltd., 310012 Hangzhou, China

Academic Editor: Dapeng Zhang < zhangdapeng@gdou.edu.cn>

Received: 7 August 2024; Revised: 30 August 2024; Accepted: 31 August 2024; Published: 5 September 2024

Abstract: Excessive air gaps between conductors and other components can occur due to wind-induced swing, potentially causing flashover or even tripping, thereby threatening the stable and safe operation of the power grid. Therefore, accurate calculation of conductor wind-induced swing response is fundamental to wind-resistant design. This paper reviews the main calculation methods for conductor wind-induced swing response, discussing the application and improvement of equivalent static wind loads in simplified static models. The impact of vertical wind load and important conclusions regarding multi-dimensional equivalent static wind loads are also highlighted. This review summarizes significant conclusions from studies on conductor wind-induced swing response, identifies inadequacies in existing research regarding the reasonable simplification of background factors and the influence of height parameters, and points out the lack of simplified calculation methods for wind-induced swing responses under combined horizontal and vertical wind loads.

Keywords: Transmission line; Wind-induced swing; Simplified calculation; Equivalent static wind load; Vertical wind load

1. Introduction

With continuous technological and economic development, global advancements in ultra-high voltage (UHV) transmission technology have been significant. In 2009, the world's first commercial 1000 kV UHV alternating current (AC) transmission line, the

Citation: Gu Y., Zhang Y. A Review of Wind-Induced Swing Response Calculations for Transmission Conductors. Eng. Solut. Mech. Mar. Struct. Infrastruct., 2024, 1(3), doi: 10.58531/esmmsi/1/3/10

ISSN/© By the Author(s) 2024, under the CC BY-NC-ND license (http://creativecommons.org/licenses/by-nc-nd/4.0

Jingdongnan-Nanyang-Jingmen project, was successfully commissioned. By 2023, China had constructed and put into operation a total of 37 UHV transmission lines, comprising 20 direct current (DC) and 17 alternating current lines. However, as the power grid system becomes increasingly inclusive, especially to improve electricity access in remote areas, the construction of transmission lines faces more complex conditions, posing greater challenges and threats to the power transmission system. In 2019, Typhoon Lekima made landfall in Wenling City, Zhejiang Province, resulting in the power outage of 4,330 power lines of 10 kV and above and 72 substations of 35 kV and above across six provinces. Among these, the Zhejiang power grid saw 23 of its 500 kV lines damaged and out of service, accounting for 30% of the province's 500 kV lines. This disaster inflicted a significant blow to social and economic development.

As the primary carrier of electrical transmission, conductors are susceptible to displacement from their initial positions under adverse ice and wind conditions, leading to a phenomenon known as wind-induced swing. Excessive swing displacement can reduce the distance between conductors, transmission tower components, or surrounding structures. When this distance does not meet critical electrical clearance requirements, air breakdown can occur, resulting in flashover and tripping incidents. These flashover incidents have a high frequency of occurrence and a low reclosing rate, making them one of the main threats to the stable operation of transmission lines.

To ensure the safe and stable supply of electricity, it is essential to accurately assess the wind-induced response of iced transmission tower-line systems. This is particularly important in mountainous terrains, where complex topographical and climatic conditions often lead to intricate wind field environments. Therefore, refined modeling and analysis of transmission lines and wind loads are necessary. Developing more rational methods for calculating the wind-induced swing response and wind resistance capacity of transmission lines is crucial to ensure their stable operation and reliability under harsh climatic conditions.

The study of wind-induced swing responses of transmission line conductors initially relied on field observations. Tsujimoto K. et al. [1] conducted a three-year full-scale observation on an independent span, performing frequency domain analysis based on the collected wind speed data. Similarly, Hiratsuka et al. [2] observed the swing angles of transmission line conductors under various wind speeds. However, such field observations and full-scale tests are expensive and inconvenient for controlling specific parameters. Consequently, with the rapid advancement in computational capabilities and finite element software, both domestic and international studies have predominantly shifted to the finite element method for simulating wind-induced swing responses. These studies typically employ time domain analysis [3-10] and frequency domain analysis [11-12] for numerical simulations.

Both time-domain and frequency-domain analyses involve the finite element method, which requires time-consuming and complex modeling and matrix computations, making it more suitable for research contexts. In contrast, simplified static models are predominantly used in engineering practice due to their ease of computation and efficiency. Additionally, equivalent static theories based on frequency-domain methods and statistical approaches

can account for dynamic amplification effects and spatial correlations of wind loads, enabling static models to achieve a level of accuracy comparable to that of finite element methods.

This paper reviews the calculation methods for conductor wind-induced swing responses, summarizing the development and refinement of equivalent static theories for wind loads in static models. It also discusses research on conductor swing responses under both horizontal and vertical wind loads. The paper explores the challenges in studying swing responses, highlights key findings and limitations, and suggests directions for future research.

2. Calculation of Wind-induced Swing Response

2.1 Finite Element Time Domain Analysis

Finite element time domain analysis involves dividing the conductor into multiple elements. Time history simulations of multi-point fluctuating wind speeds are then conducted as shown in Equation. 1, with wind load vectors formed based on the quasi-steady assumption. The wind-induced swing response is subsequently obtained by iteratively solving the nonlinear motion equations of the conductor as shown in Equation. 2. This approach allows for a more accurate consideration of the nonlinearities in load, material properties, and responses by employing refined finite element models and applying loads with varying distributions as necessary. This results in more realistic and precise analysis outcomes.

$$\tilde{W}_j\left(y_j, z_j, t\right)=\sqrt{2(\Delta\omega)}\sum_{m=1}^{j}\sum_{l=1}^{N}H_{jm}\left(\omega_{ml}\right)\cos\left(\omega_{ml}t-\theta_{jm}\omega_{ml}+\Phi_{ml}\right) \tag{1}$$

$$\mathbf{M}\ddot{\mathbf{Y}}+\left(\mathbf{C}_{\text{str}}+\mathbf{C}_{\text{aero}}\right)\dot{\mathbf{Y}}+\mathbf{K}\mathbf{Y}=\mathbf{F} \tag{2}$$

Regarding the selection of conductor elements, McClure et al. [13] utilized two-node (linear) isoparametric truss elements for conductor modeling. Shehata et al. [14] addressed the geometric nonlinearity of the conductor by employing two-dimensional curved beam elements. Stengel et al. [15] used cable elements, which enabled accurate reproduction of the conductor's static catenary configuration with a reduced number of elements. To account for the influence of transmission towers on the conductor's swing response, Zhou et al. [16] developed a tower-line system for finite element time domain analysis. Shehata et al. [14] modeled the tower using three-dimensional linear elastic frame elements. Hamada et al. [17] further refined this approach by incorporating a three-dimensional nonlinear spring system to simulate the stiffness of the tower and insulator strings, as illustrated in Figure. 1.

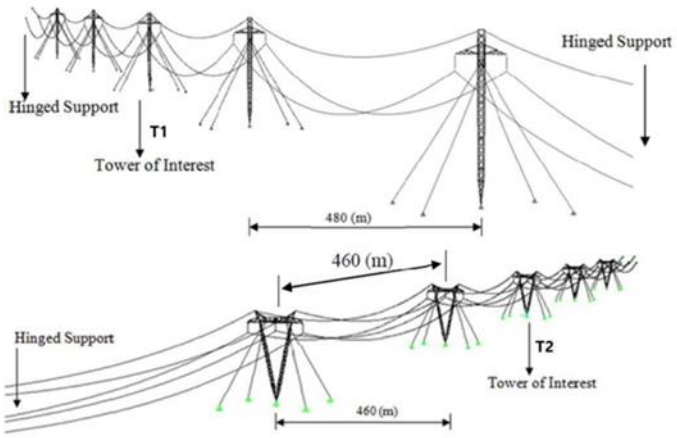

Figure. 1. Geometry of the modelled guyed transmission lines [17]

However, Davenport [18] posited that the frequency of the tower is significantly higher than that of the conductor, rendering the impact of tower vibrations on the conductor's wind-induced swing response negligible. As a result, many researchers have concentrated their analyses on the insulator string-conductor coupling model. Current standards also tend to overlook the effects of tower vibrations.

Due to the significant flexibility of transmission conductors, large displacements and velocities occur during motion, making aerodynamic damping highly influential on the dynamic response of the conductors. In time domain analysis, the impact of aerodynamic damping is typically considered by introducing the relative velocity between the conductor and the incoming flow [1,15]. Wind loads are calculated using the relative velocity, as shown in the Equation. 3. The last term is often considered negligible. The first term represents the wind load on a stationary conductor due to the incoming flow, while the second term, which is proportional to the conductor's velocity, accounts for the aerodynamic damping caused by the conductor's motion relative to the flow.

$$\frac{1}{2}\rho C_d A\left(W-\dot{Y}\right)^2=\frac{1}{2}\rho C_d AW^2-\rho C_d AW\dot{Y}+\frac{1}{2}\rho C_d A\dot{Y}^2 \tag{3}$$

The finite element time domain analysis process is intuitive and yields accurate and reliable results. It supports parametric analysis tailored to specific research needs and has become a benchmark for validating the accuracy of other computational methods. Liu et al. [7] and Yan et al. [8,19] utilized this method to perform finite element simulations of the wind-induced swing response of transmission lines under random wind fields. Their findings revealed that traditional calculation methods recommended by the Code for Electrical Design of Overhead Transmission Line [20] significantly underestimated the wind-induced swing response. This led to the adoption of a dynamic wind load factor to account for the amplification effects of fluctuating winds. Lou et al. [21] employed the vector synthesis method to reconstruct the three-dimensional transient wind field of moving downburst. They used instantaneous wind attack angles to describe the vertical wind direction angles over time and conducted numerical simulations of the wind-induced swing of transmission conductors.

2.2 Finite Element Frequency Domain Analysis

Davenport [22] was the first to categorize structural responses into mean, background, and resonance components based on their frequency characteristics, thereby facilitating calculations that are based on more clearly defined physical meanings. However, due to the significant nonlinear nature of conductor dynamic responses, direct application of frequency domain analysis is not feasible. To address this issue, Yasui et al. [23] and Haddadin et al. [24] proposed a two-step approach for frequency domain analysis. This method involves first determining the mean response of the conductor under steady wind loads through nonlinear analysis. Since the fluctuating wind load constitutes a relatively small portion of the total wind load, the fluctuating response can be approximated as linear. Consequently, frequency domain analysis is used to efficiently solve the linear component of the response [11]. The key equations are presented in Equation. 4 through Equation. 6.

$$S_{yy}(\omega)=\sum_{j=1}^{n_0}\sum_{k=1}^{n_0}\phi_{Y_j}\phi_{Y_k}H_j^*(\omega)H_k^*(\omega)S_{pp}(\omega) \tag{4}$$

$$\sigma_y=\sqrt{\int_0^\infty S_{yy}(\omega)\mathrm{d}\omega} \tag{5}$$

$$Y_{\max}=\bar{Y}+g\sigma_y \tag{6}$$

Similarly, Zhang et al. [25] introduced the linearization assumption of wind speed and fluctuating wind pressure, proposing a simplified method for frequency domain analysis of wind-induced vibrations in tower-line systems. The effectiveness of this simplified approach was validated through comparisons with ADINA results. Wang et al. [26] derived the frequency domain solution for dynamic tension in the insulator string-conductor coupling system. Lou et al. [4,11-12] employed both time domain and frequency domain analyses to perform incident analysis of wind-induced flashover events on real high-voltage transmission lines. They conducted parametric analyses to assess the impact of structural parameters on wind-induced responses and found that the frequency domain method provided computational accuracy comparable to the time domain analysis. Additionally, their research explored the effects of multiple vibration modes and their combinations on conductor wind-induced swing, emphasizing the importance of mode interaction terms [27].

Frequency domain analysis can achieve computational accuracy comparable to time domain analysis with fewer vibration mode combinations and does not require time-consuming wind field simulations or iterative nonlinear equation solving processes. This approach, therefore, shortens the computation time to some extent. Additionally, frequency domain analysis forms the basis for the equivalent static wind load theory, allowing for the consideration of dynamic responses using static models. Detailed information on this will be presented in Chapter 3.

2.3 Simplified Models

To conserve computational resources and reduce calculation time, researchers have introduced various simplifications and equivalent principles, leading to the development of simplified models for analysis. The main simplified models are shown in Figure. 2. Dua et al. [28] reduced computational complexity by segmenting transmission towers to determine

their equivalent axial, bending, torsional, and shear stiffnesses, thus representing them as beam elements with uniform stiffness and material properties. Figure. 2(a) shows a comparison of the modes of key nodes of the transmission tower before and after equivalence. Aboshosha et al. [29] developed a conductor-insulator string model for multi-span transmission lines, dividing the system at conductor attachment points and treating each span individually without further subdivision. Based on the static equilibrium equations for the conductor and insulator string, and assuming a constant conductor length, they derived a set of nonlinear coupled equations for attachment point reactions and displacement components, which were solved using iterative methods. Subsequently, a further simplification was proposed by modeling secondary towers as a combination of roller supports and linear springs, thereby reducing the number of equations in the system [30], as illustrated in Figure. 2(b). When compared with finite element methods for scenarios such as downbursts and typhoons, this approach demonstrated improved accuracy and computational efficiency. The primary advantage of this method lies in its ability to replace detailed subdivisions with load and internal force integrations for each span, effectively reducing the dimensionality of the solved matrix.

Additionally, Tsujimoto K et al. [1] introduced a spring-mass model that simplifies the conductor into a series of mass elements connected by massless springs, as shown in Figure. 2(c). Wang et al. [26] developed a spring-pendulum model to simulate the first-order out-of-plane and in-plane vibration responses of the conductor, as illustrated in Figure. 2(d). Furthermore, Hu et al. [31-33] enhanced the traditional finite element method used in time domain analysis by proposing a multi-rigid-body model for calculating the wind-induced swing responses of continuous-span overhead transmission lines. The schematic diagram of the model is shown in Figure. 2(e), which significantly reduces the number of elements required for computation.

Although the aforementioned models reduce computational complexity to some extent, they still rely on finite element methods, which involve complex and time-consuming line modeling and matrix solving processes. Consequently, these models are more of a simplified numerical approach rather than a practical engineering simplification. In engineering practice, static analysis methods are commonly used for structural wind resistance design in the field of wind engineering. Below are several practical static models for wind-induced swing responses proposed by researchers.

Clapp et al. [34] proposed an accurate static method for calculating the wind-induced swing angle of insulator strings, considering their non-rigidity. This method involves establishing static equilibrium equations starting from the lower end of the insulator string and progressively determining the wind-induced angle upwards. This approach provides the wind-induced response at various points along the insulator string. In addition, many studies [2,4,35] utilize a simplified static equilibrium equation, as shown in Equation. 7, to calculate the wind-induced swing angle of the planes of conductor or insulator strings. This method simplifies the insulator string-conductor coupling system into a rigid rod-particle model, concentrating the conductor's gravitational and horizontal wind loads at the end of the insulator string, as illustrated in Figure. 2(f). The wind-induced angle of the insulator string is then calculated based on static equilibrium relationships to verify the minimum air

gap between the insulator string and the tower or other structures. This method is referred to as the rigid rod method in Chinese regulations [20]. Research indicates that while Clapp's method provides a more accurate overall displacement distribution for the insulator string, the calculation accuracy for displacements at conductor attachment points is nearly the same between the two methods.

$$\tan\theta = \frac{W_c + W_s/2}{G_c + G_s/2} \quad (7)$$

Due to its simplicity and clarity, the rigid rod method is widely adopted in standards [36-38] across various countries for calculating wind-induced swing responses. As static models do not account for dynamic response characteristics, employing equivalent static wind loads to address the dynamic effects of fluctuating winds has become an effective approach in wind resistance design.

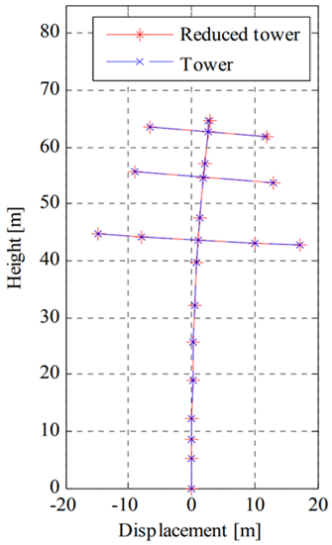

(a) Equivalent tower model [28]

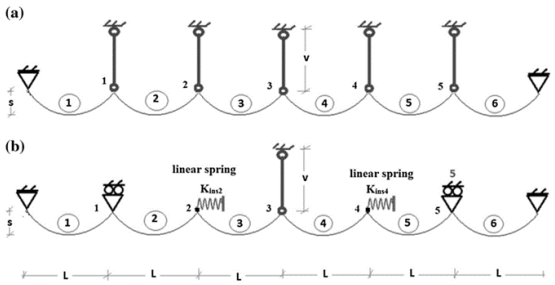

(b) Multi-span conductor-insulator string model [30]

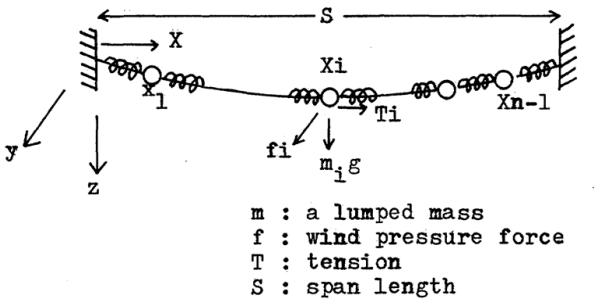

(c) Spring-mass simulation model [1]

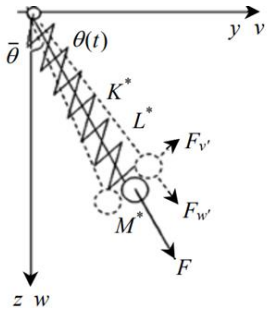

(d) Spring pendulum model [26]

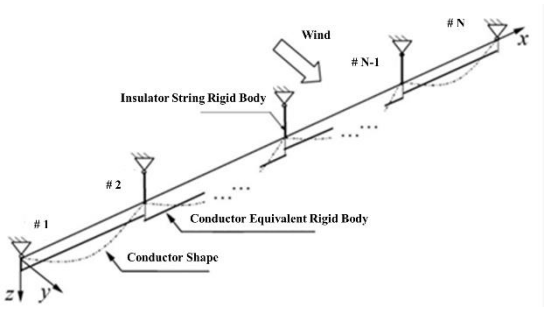

(e) Multi-rigid-body model [31]

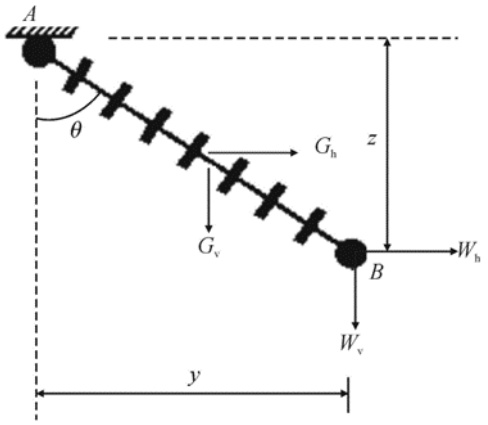

(f) The model of rigid rod method [4]

Figure. 2. Simplified models for calculating wind-induced conductor swing

3. Equivalent Static Wind Load Theory

3.1 Theory Proposition and Improvement

Davenport [22] proposed the gust load factor method, defining the gust load factor as the ratio of the expected maximum response to the mean response. By introducing random vibration theory and employing joint acceptance functions, as shown in Equation. 8 through Equation. 9, to calculate the background and resonance factors separately, the peak fluctuating response can be expressed as a linear combination of the background and resonance components [39-40]. The gust load factor method provides a closed-form solution for equivalent static wind loads, comprehensively considering the dynamic amplification effect and spatial correlation of fluctuating wind loads, thereby offering a physically meaningful computational theory for wind resistance design. However, since the gust load factor involves the ratio to the mean response and load, it encounters difficulties when dealing with crosswind, vertical and torsional loads or responses, whose means are zero, rendering the ratio meaningless [41]. To derive the analytical expressions for the background factor or the variance of the background response, scholars have made a series of improvements. The respective analytical expressions are listed in Table 1.

$$J_Z(n)=\sqrt{3\int_0^1\int_0^1\frac{\bar{V}(Z)}{\bar{V}_1}\frac{\bar{V}(Z^1)}{\bar{V}_1}ZZ^1\mathrm{e}^{-C|Z-Z^1|}\mathrm{d}Z\mathrm{d}Z^1} \tag{8}$$

$$J_H(n)=\sqrt{\int_0^1\int_0^1\mathrm{e}^{-C|x-x^1|}\mathrm{d}x\mathrm{d}x^1} \tag{9}$$

Holmes [42-43] proposed the covariance integration method, which uses influence lines and wind pressure covariance instead of mode-based joint acceptance functions to calculate the background component. Loredo-Souza et al. [46] calculated the mean and background components of the response using the influence line and statistical method, while the resonance component was still calculated using mode-based joint acceptance functions. The effectiveness of this method was validated based on wind tunnel test results [47-48]. Additionally, Holmes [44-45] introduced a generalized format of the gust response factor (or dynamic response factor) applicable to various standards, addressing issues

related to differences in the selected moving average wind speed durations across different standards.

Holmes [49-50] also noted that the mean, background, and resonance components of equivalent static wind loads each have different load distribution forms. The resonance component shares the same distribution as inertia loads, while the background load distribution depends on the spatial correlation of fluctuating wind pressure and the form of the structure's load influence line. The effective static load distributions are illustrated in Figure. 3. Therefore, calculating the equivalent static wind load using the same distribution as the mean wind load in the gust response factor method might lead to response misestimation, especially for structures with complex load influence lines.

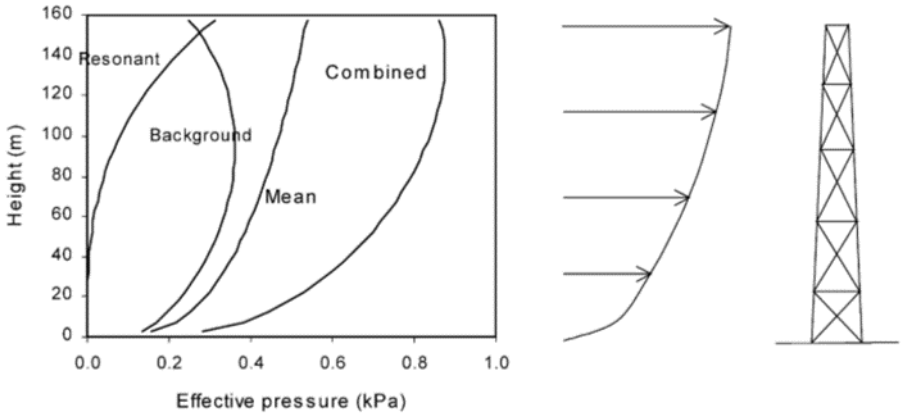

Figure. 3. Effective static load distributions [49]

Kasperski et al. [51-52] proposed the Load Response Correlation (LRC) method, which calculates the background response by analyzing the most likely load distribution for a given target response. Additionally, Blaise et al. [53-54] integrated the equivalent static wind loads for various responses and used singular value decomposition to obtain the principal static wind load. This approach facilitated the reconstruction of the gust envelope and extended the LRC method into a more general Displacement Response Correlation (DRC) method. The DRC method comprehensively considers both background and resonance components and is applicable to non-Gaussian response scenarios.

The LRC method accounts for the spatial correlation of fluctuating wind loads by applying different reduction factors to the fluctuating wind loads at various spatial positions on the structure. However, this increases computational complexity. To address this issue, Chen et al. [55] proposed the Gust Loading Envelope (GLE) method. The GLE method simplifies the calculation of equivalent static wind loads by applying a uniform reduction factor, based on the background factor, to the fluctuating wind loads at all spatial positions of the structure. This approach streamlines the process while still considering the key effects of fluctuating wind loads.

Table 1. The proposed analytical expressions concerning the background response

Author	Background Factor or Variance of the Background Response
Davenport [22]	$\frac{16}{3r}(1+\alpha)^2\int_{-\infty}^{\infty}\lvert J_Z(n)\rvert^2\lvert J_H(n)\rvert^2\frac{nS_V(n)}{\bar{V}_1^2}\mathrm{d}\log_e n$

Holmes [42]	$\sqrt{\sum_{i=1}^{N}\sum_{j=1}^{N}\overline{p_i'p_j'}\beta_i\beta_j\Delta A_i\Delta A_j}$
Loredo-Souza et al. [46]	$2qC_{\mathrm{D}}dI_v\sqrt{\int_0^l\int_0^l\exp\left(-\Delta x/L_v\right)i\left(x\right)i\left(x'\right)\mathrm{d}x\mathrm{d}x'}$
Kasperski et al. [52]	$\frac{\sigma_{r_ip_k}^2}{\sigma_{r_i}\sigma_{p_k}}$
Chen et al. [55]	$\frac{\sqrt{\int_0^H\int_0^H\mu_x\left(z_1\right)\mu_x\left(z_2\right)R_{P_{xx}}\left(z_1,z_2\right)\mathrm{d}z_1\mathrm{d}z_2}}{\int_0^H\mu_x\left(z\right)\sqrt{R_{P_x}\left(z\right)}\mathrm{d}z}$

3.2 Application to Conductor Wind-Induced Swing Calculation

Since wind speeds at different points on a structure are not fully coherent in space, peak wind loads do not occur simultaneously. Designing for wind resistance based on extreme wind loads can lead to an overestimation of the response [42,56-57]. Therefore, accurately calculating the background response and its spatial correlation is crucial for assessing conductor responses. For flexible transmission conductors, the wind-induced swing response is dominated by the mean and background components due to significant aerodynamic damping, while the resonance response can be neglected [3,5,46]. Studies by Aboshosha et al. [9] also indicate that the resonance component of the wind-induced response of transmission conductors is minimal under both downburst and synoptic wind conditions, making the quasi-static method a reasonable approach for calculations.

To achieve sufficient simplification in engineering applications, international standards and researchers have proposed various simplified expressions for the span reduction factors or the background factor, as listed in Table 2. Standards such as IEC 60826-2017 [58], and JEC-127-1979 [59] employ span reduction factors to account for the difference between expected response and extreme wind load response [3,60-63]. In contrast, ASCE-74 [37] uses background factors to reduce the effect of partially coherent fluctuating wind.

In the framework of the GRF method, the background factor is described by the joint acceptance function of the background component. In the frameworks of the LRC and GLE methods, the background factor serves as the wind load reduction factor. Each of these approaches has clear physical significance but involves complex double integration calculations. Therefore, simplifying the calculation of the background factor is of paramount importance.

To address this, Holmes [64] proposed a simplified formula for the background factor based on quasi-steady assumptions for variable-section lattice towers. This formula calculates the background factor at various points along the tower by considering the tower height, the height of the wind load, and the integration length scale. Building on this, Chen et al. [55] incorporated nonlinear wind load profiles and load influence lines, noting that the background factor is insensitive to the wind profile exponent coefficient. They proposed an expression for the background factor suitable for structures with power-law load influence lines. Solari [65] introduced simplified formulas for the background factor for point,

vertical, and horizontal structures. Additionally, Dyrbye et al. [66] analytically simplified the background factor for slender structures by replacing complex double integrals with two simpler single integrals. Blaise et al. [67] further derived expressions for the background factor related to higher-order statistics, such as variance, skewness, and kurtosis, under non-Gaussian wind pressure effects. The DL/T 5582-2020 standard [20] adopted this framework and converted the background factor into an equivalent span reduction coefficient for calculations.

Table 2. The proposed simplified expressions for the span reduction factors or the background factor

Author or Code	Span Reduction Factor or Simplified Background Factor
IEC 60826-2017 [58]	$4\times10^{-10}L^3-5\times10^{-7}L^2-10^{-4}L+1.04035$
JEC-127-1979 [59]	$0.5+40/L$
ASCE-74 [37]	$1/\sqrt{1+0.8S/L_s}$
Holmes [64]	$1/\sqrt{1+(h-s)/(3.5^z L_u)}$
Chen et al. [55]	$1/\sqrt{1+(h-s)/[(2.5+\beta_0)L_u]}$
Solari [65]	$24/(1.06+0.65\lambda-0.23\lambda^2)$ (point-like structures) $17.18/(1+0.16\lambda)$ (vertical structures) $24/\sqrt{1.39+0.63\lambda}$ (horizontal structures)
Dyrbye et al. [66]	$\int_0^1 h(s,f)\sqrt{\mathrm{Coh}(y_1,y_2,f,U)}\mathrm{d}s,\quad h(s,f)=2\int_0^{1-s} g(y,f)g(y+s,f)\mathrm{d}y$
Blaise et al. [67]	$\frac{2}{3\phi}-\frac{1}{\phi^2}+\frac{2}{\phi^4}-e^{-\phi}\left(\frac{2}{\phi^3}+\frac{2}{\phi^4}\right)$
DL/T 5582-2020 [20]	$\frac{\sqrt{12L_xL_p^3+54L_x^4-36L_x^3L_p-72L_x^4\exp(-L_p/L_x)+18L_x^4\exp(-2L_p/L_x)}}{3L_p^2}$

This underscores the challenge in evaluating wind-induced responses accurately, particularly in obtaining precise background factors in a straightforward manner. Current simplified formulas are typically derived from horizontal coherence functions, determined solely by horizontal span and integral length scale, and often neglect the vertical correlation of wind speeds and the impact of height variations on spatial correlation. In reality, greater elevation often means that conductors are exposed to a more uniform wind field, resulting in higher spatial correlation of wind loads. Ignoring height effects can therefore lead to incorrect estimates of structural responses.

4. Wind-Induced Swing Response of Conductors Under Horizontal and Vertical Wind Loads

For mountain transmission lines or those affected by downbursts, conductors are subjected not only to horizontal wind loads but also to vertical wind loads, resulting in

two-dimensional wind loading. Vertical wind loads are primarily caused by two factors: first, updrafts or downdrafts induced by microtopography or meteorological conditions, and second, aerodynamic lift generated by asymmetrical ice-covered cross-sections.

4.1 Updrafts and Downdrafts Research

Research indicates that terrain effects can lead to significant localized vertical wind, which notably impact the wind-induced swing response of transmission lines. Hung et al. [68] conducted field observations and response analyses of practical transmission lines in mountainous terrains, finding that the vertical component of turbulence intensity can be as much as half of the horizontal component, resulting in substantial vertical responses due to two-dimensional wind loads. Xu et al. [69] examined the swing response of jumper lines under three-dimensional fluctuating wind speeds in microterrain, noting that vertical wind speeds can reach up to 35% of the horizontal wind speed. They emphasized the importance of considering vertical wind speeds at ridge locations, as the combination of horizontal wind and updrafts further amplifies wind-induced swing responses. Liu et al. [70] investigated the effects of isolated mountain terrain on wind fields and wind-induced swing response characteristics. They found that downflows aligned with the mountain range can pass smoothly to the sides, making vertical wind speeds negligible, whereas vertical wind speeds in the direction perpendicular to the mountain range are more significant and should be factored into the design. Liu et al. [71] further analyzed the effects of variations in mountain length, slope, and spacing on wind-induced swing responses in terrain conditions such as passes and valleys, providing a quadratic regression equation that relates terrain factors to the increase in swing angle.

Additionally, Lou et al. [72] analyzed the impact of mountain wind fields on the wind-induced swing of transmission lines by combining wind tunnel test results with the Proper Orthogonal Decomposition (POD) method to simulate fluctuating wind speeds. Their findings indicated significant updrafts at specific local positions along the line due to airflow climbing slopes, which had a substantial impact on the vertical wind-induced swing displacement of conductors, while the horizontal displacement was minimally affected. Figure. 4 illustrates the wind field model in various mountainous terrains as investigated by Liu and Lou. Du et al. [73] conducted a parametric analysis of wind-induced swing responses under two-dimensional inflow conditions and introduced an amplification factor to correct for the influence of vertical winds on equivalent static wind loads. They found that the vertical component of the wind-induced swing response was less sensitive to horizontal fluctuating winds, while the horizontal component was almost equally sensitive to fluctuating winds in both directions. Zhou et al. [74] considered the funnel effect in valley areas and used computational fluid dynamics (CFD) methods to determine wind speed distribution within valleys. They also performed dynamic analysis of transmission lines considering two-dimensional wind loads and rain loads.

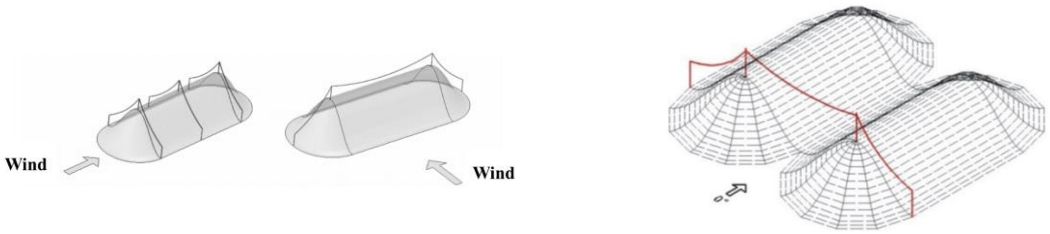

(a) Model analyzed by Liu [70] (b) Model analyzed by Lou [72]

Figure. 4. Mountainous terrain model and definition of wind direction

Regarding vertical wind loads caused by meteorological conditions, Aboshosha et al. [29] proposed a multi-span transmission line model for conductor-insulator strings, which is applicable to conductors under arbitrary distributions of horizontal and vertical loads. They analyzed conductor displacement responses under downburst and typhoon conditions. Hamada et al. [17] employed a nonlinear three-dimensional analysis method that considers the effects of vertical and lateral wind speeds in tornadoes, as well as the coupling of vertical and lateral responses.

4.2 Aerodynamic Effects of Iced Conductors Research

Research on the combined effects of drag and lift on wind-induced swing responses of iced conductors is relatively scarce. Zhang et al. [75-76] conducted wind tunnel tests on the aerodynamic characteristics of connected ellipse iced conductors. They compared the effects of connected ellipse ice and separated ellipse ice on the wind-induced swing responses of conductors and considered changes in insulator string height due to wind-induced swing, making improvements to the rigid rod method. The results indicated that the average drag coefficient of the connected ellipse iced conductors was generally higher, and the average lift coefficient was significantly higher than that of the separated ellipse iced conductors, resulting in more pronounced wind-induced swing responses of the insulator string and conductors. Lou et al. [77] analyzed the effects of ice shape and wind attack angle on the wind-induced swing responses of conductors based on wind tunnel test results for crescent-shaped and D-shaped iced conductors. They pointed out significant discrepancies between the calculation results of the standard and the analysis.

4.3 Equivalent Calculation Methods for Multi-Dimensional Loads

For structures with complex geometries that may exhibit three-dimensional coupled modes and responses, Chen et al. [39] addressed the correlation between wind loads in different directions and the effects of multi-modal coupling. They proposed a framework for calculating equivalent static wind loads under three-dimensional coupled wind loads. Liang et al. [78] developed an equivalent static wind load model specifically for symmetric high-rise buildings. This model incorporates coupling effects in along-wind, across-wind, and torsional directions, while also accounting for higher-order modal contributions. It aims to predict the coupled responses of high-rise buildings with complex modal shapes and uneven mass distribution. They noted significant differences between their results and the equivalent static wind loads recommended by Chinese codes.

Luo et al. [79-80] introduced non-Gaussian factors to account for the non-Gaussian characteristics of wind-induced responses. By using contribution coefficients, they correlated multiple single-objective equivalent static wind loads to develop a three-dimensional multi-objective equivalent static wind load model for flexible high-rise buildings with complex geometries. This model allows for accurate estimation of multiple target responses and compares the applicability of the LRC method, GLE method, and multi-objective equivalent method. For simplified calculations, Hu et al. [81] proposed a simplified formula for calculating the mean wind-induced swing response of insulator strings under slope wind attack angle, as shown in Equation. 10.

$$\bar{\theta} = \arctan \frac{\left(\frac{1}{2}\phi \bar{V}_{\mathrm{I}}^2 + \psi L_{\mathrm{H}} \bar{V}^2\right)\cos\varphi}{mgL_{\mathrm{V}} + \frac{1}{2}M_{\mathrm{I}}g + \left(\frac{1}{2}\phi \bar{V}_{\mathrm{I}}^2 + \psi L_{\mathrm{H}} \bar{V}^2\right)\sin\varphi} \tag{10}$$

In mountainous terrains, vertical winds and ice accretion on conductors may occur simultaneously. However, there is currently a lack of research on the combined effects of these factors on the wind-induced swing response of transmission lines. The existing rigid rod method typically simplifies the incoming flow to horizontal wind loads, failing to account for the potential vertical wind effects in complex terrains or the lift forces caused by asymmetrical ice-covered sections. Further research is needed on the equivalent static wind load response of conductors under multi-dimensional wind loads.

5. Conclusions

This paper reviews the calculation methods for the wind-induced swing response of transmission conductors. Both time-domain and frequency-domain analyses, as well as several main simplified models, are introduced. The development and improvement of equivalent static wind load theory, which compensates for the neglect of dynamic characteristics of wind loads in simplified static models, are discussed in detail. Studies on the impact of updrafts, downdrafts, and aerodynamic lift on swing response have also yielded significant conclusions. From this review, the following conclusions can be drawn:

(1) Time-domain analysis, while highly accurate, requires complex and time-consuming wind speed simulations and iterative calculations. It is primarily used in scientific research and serves as a benchmark for validating the accuracy of other methods. The rigid rod method, being the simplest simplified model, is more convenient and offers relatively high accuracy, making it the main calculation method used in engineering.

(2) By combining frequency domain analysis and statistical theory, the dynamic characteristics of wind loads can be considered to obtain equivalent static wind loads. This allows the rigid rod method to achieve accuracy comparable to the finite element method. The challenge in calculating equivalent static wind loads lies in accurately determining and reasonably simplifying the background factor.

(3) In existing simplified formulas for the background factor of wind-induced swing response, only the influence of horizontal span is considered, neglecting the impact of conductor height on the characteristics of fluctuating wind. This omission may lead to inaccuracies in calculating wind-induced swing responses for lines with significant height

variations in mountainous terrains. The effect of height parameters on the background factor requires further investigation.

(4) Vertical wind and aerodynamic lift can significantly impact the wind-induced swing of conductors in the vertical direction. However, existing studies concerning the rigid rod method generally focus on horizontal wind loads, neglecting the effects of vertical wind loads. Simplified methods for analyzing wind-induced swing responses under two-dimensional wind loads and calculating equivalent static wind loads are still lacking.

Conflict of interest: The authors declare that they have no known competing financial interests or personal relationships that could have appeared to influence the work reported in this paper.

References:

1. K. Tsujimoto, et al. Investigation of conductor swinging by wind and its application for design of compact transmission line. IEEE Transactions on Power Apparatus and Systems. 1982; (11): 4361-4369.
2. Satoshi Hiratsuka, et al. Field test results of a low wind-pressure conductor. In Proceedings of IEEE Region 10 International Conference on Electrical and Electronic Technology. 2001; 2: 664-668.
3. M. Matheson, and J. Holmes. Simulation of the dynamic response of transmission lines in strong winds. Engineering Structures. 1981; 3(2): 105-110.
4. Zhongbing Lyv, et al. Analysis of one UHVAC transmission line windage yaw. High Voltage Apparatus. 2019; 55(1): 170-177.
5. Wenjuan Lou, et al. Windage yaw dynamic analysis methods for transmission lines considering aerodynamic damping effect. J. Vib. Shock. 2015; 34(6): 24-29.
6. Shuang Zhao, et al. Dynamic windage yaw angle and dynamic wind load factor of a suspension insulator string. Shock and Vibration. 2022; (1): 6822689.
7. Xiaohui Liu, et al. Numerical simulation of windage yaw of 500KV UHV transmission lines. Eng. Mech. 2009; 33: 244-249.
8. Bo Yan, et al. Research on dynamic wind load factors for windage yaw angle of suspension insulator strings. Engineering Mechanics. 2010; 27(1): 221-227.
9. Haitham Aboshosha, et al. Dynamic response of transmission line conductors under downburst and synoptic winds. Wind and Structures. 2015; 21(2): 241-272.
10. Xuan Min, et al. The influence of transmission line arrangements on the swing angle of suspension insulator string. Electric Power. 2013; 46(1): 69:74.
11. Wenjuan Lou, et al. Dynamic wind-induced swing response and parameters' influence analysis of UHV transmission lines. China Civil Engineering Journal. 2019; 52: 41-49.
12. Yue Yang. Study on calculation of conductor swinging under fluctuating wind loads [D]. Hangzhou. China. 2015.

13. G. McClure, et al. Modeling the structural dynamic response of overhead transmission lines. Computers & Structures. 2003; 81(8-11): 825-834.
14. A. Shehata, et al. Finite element modeling of transmission line under downburst wind loading. Finite elements in analysis and design. 2005; 42(1): 71-89.
15. Dominik Stengel, and Milad Mehdianpour. Finite element modelling of electrical overhead line cables under turbulent wind load. Journal of structures. 2014; (1): 421587.
16. Linshu Zhou, et al. Numerical study on dynamic swing of insulator string in tower-line system under wind load. In 2012 Asia-Pacific Power and Energy Engineering Conference. 2012: 1-4.
17. Ahmed Hamada, and Ashraf El Damatty. Behaviour of transmission line conductors under tornado wind. Wind and Structures. 2016; 22(3): 369-391.
18. Alan Davenport. Gust response factors for transmission line loading. In Wind engineering. 1980: 899-909.
19. Bo Yan, et al. Numerical study on dynamic swing of suspension insulator string in overhead transmission line under wind load. IEEE Transactions on power delivery. 2009; 25(1): 248-259.
20. Code for electrical design of overhead transmission line: DL/T 5582-2020. Beijing: China Planning Press. 2020.
21. Wenjuan Lou, et al. Calculation method of wind-induced oscillation of transmission line under moving downburst. Proceedings of the CSEE. 2015; 35(17): 4539-4547.
22. Alan Davenport. Gust loading factors. Journal of the Structural Division. 1967; 93(3): 11-34.
23. H. Yasui, et al. Analytical study on wind-induced vibration of power transmission towers. Journal of wind engineering and industrial aerodynamics. 1999; 83(1-3): 431-441.
24. S. Haddadin, et al. Sensitivity of wind induced dynamic response of a transmission line to variations in wind speed. In Proc. Resilient Infrastruct. 2016: 1-8.
25. Chuancai Zhang, and Qiang Guo. A simplified frequency domain analysis method for wind-induced vibration response of transmission tower-line system. Chiniese Journal of Applied Mechanics. 2022; (5): 782-786.
26. Dahai Wang, et al. Dynamic tension model for wind-induced vibration of long spanned transmission line. In Proceedings of the CSEE. 2009; 29(28): 122-128.
27. Wenjuan Lou, et al. Response characteristics and frequency-domain calculation method of dynamic wind-induced deflection of transmission lines. High Voltage Eng. 2017; 43(5): 1493-1499.
28. Alok Dua, et al. Dynamic analysis of overhead transmission lines under turbulent wind loading. Open Journal of Civil Engineering. 2015; 5(4): 359-371.
29. Haitham Aboshosha, and Ashraf El Damatty. Effective technique to analyze transmission line conductors under high intensity winds. Wind Struct. 2014; 18(3): 235-252.
30. Haitham Aboshosha, and Ashraf El Damatty. Engineering method for estimating the reactions of transmission line conductors under downburst winds. Engineering Structures. 2015; 99: 272-284.

31. Xin Hu, et al. Multi-rigid-body model of dynamic wind-induced deflection for overhead transmission lines. Journal of Central South University (Science and Technology). 2020; 51(12): 3465-3474.
32. Xin Hu, et al. Multi-rigid-body dynamic model and analysis for wind-induced deflection calculation of overhead lines. Journal of Vibration Engineering. 2023; 36(3): 737-747.
33. Xin Hu, et al. Sensitivity characteristics of dynamic wind-induced deflection response of insulator string on overhead lines. Journal of Vibration Engineering. 2022; 35(1): 131-139.
34. Allen Clapp. Calculation of horizontal displacement of conductors under wind loading toward buildings and other supporting structures. IEEE transactions on industry applications. 1994; 30(2): 496-504.
35. John Clair. Clearance calculations of conductors to buildings. In Proceedings of 1996 Transmission and Distribution Conference and Exposition. 1996: 493-498.
36. Australian/New Zealand Standard. AS/NZS 7000:2016 Overhead line design. Standards Australia. 2016.
37. Task Committee on Electrical Transmission Line Structural Loading. Guidelines for Electrical Transmission Line Structural Loading. Reston, VA: American Society of Civil Engineers. 2020.
38. Electrical Supply Association of Australia. ESAA C(b)1-2003 Guide-lines for Design and Maintenance of Overhead Distribution and Trans-mission Lines. Standards Australia. 2003.
39. Xinzhong Chen, and Ahsan Kareem. Coupled dynamic analysis and equivalent static wind loads on buildings with three-dimensional modes. Journal of structural Engineering. 2005; 131(7): 1071-1082.
40. John Holmes, Along wind response of lattice towers—III. Effective load distributions. Engineering Structures. 1996; 18(7): 489-494.
41. Yin Zhou, and Ahsan Kareem. Gust loading factor: New model. Journal of Structural Engineering. 2001; 127(2): 168-175.
42. J. Holmes, and R. Best. An approach to the determination of wind load effects on low-rise buildings. Journal of Wind Engineering and Industrial Aerodynamics. 1981; 7(3): 273-287.
43. R. Best, and J. Holmes. Use of eigenvalues in the covariance integration method for determination of wind load effects. Journal of Wind Engineering and Industrial Aerodynamics. 1983; 13(1-3): 359-370.
44. John Holmes, et al. Gust durations, gust factors and gust response factors in wind codes and standards. Wind and Structures. 2014; 19(3): 339-352.
45. John Holmes. Gust loading factor to dynamic response factor (1967-2002). In Symp. Preprints, Engineering, Symp. to Honor Alan G. Davenport for his. 2002; 20: 20-22.
46. A. Loredo-Souza, and A. Davenport. The effects of high winds on transmission lines. Journal of Wind Engineering and Industrial Aerodynamics. 1998; 74: 987-994.

47. A. Loredo-Souza, and A. Davenport. A novel approach for wind tunnel modelling of transmission lines. Journal of wind engineering and industrial aerodynamics. 2001; 89(11-12): 1017-1029.
48. A. Loredo-Souza, and A. Davenport. Wind tunnel aeroelastic studies on the behaviour of two parallel cables. Journal of Wind Engineering and Industrial Aerodynamics. 2002; 90(4-5): 407-414.
49. John Holmes. Effective static load distributions in wind engineering. Journal of wind engineering and industrial aerodynamics. 2002; 90(2): 91-109.
50. John Holmes, et al. A commentary on the Australian standard for wind loads AS 1170 Part 2, 1989. Australian Wind Engineering Society. 1990.
51. M. Kasperski. Extreme wind load distributions for linear and nonlinear design. Engineering Structures. 1992; 14(1): 27-34.
52. M. Kasperski, and H. Niemann. The LRC (load-response-correlation)-method a general method of estimating unfavourable wind load distributions for linear and non-linear structural behaviour. Journal of Wind Engineering and Industrial Aerodynamics.1992; 43(1-3): 1753-1763.
53. Nicolas Blaise, and Vincent Denoël. Principal static wind loads. Journal of Wind Engineering and Industrial Aerodynamics. 2013; 113: 29-39.
54. Nicolas Blaise, et al. Reconstruction of the envelope of non-Gaussian structural responses with principal static wind loads. Journal of Wind Engineering and Industrial Aerodynamics. 2016; 149: 59-76.
55. Xinzhong Chen, and Ahsan Kareem. Equivalent static wind loads on buildings: new model. Journal of Structural Engineering. 2004; 130(10): 1425-1435.
56. Wenjuan Lou, et al. Value study on span reduction coefficient and non-uniformity coefficient of wind pressure of transmission lines. Zhejiang Electric Power. 2019; 38: 72-77.
57. Feng Li, et al. Investigation of the spatial coherence function of wind loads on lattice frame structures. Journal of Wind Engineering and Industrial Aerodynamics. 2021; 215: 104675.
58. International Electrotechnical Commission (IEC). Overhead Transmission Lines – Design Criteria. 2017.
59. Japanese Electrotecnical Committee. Design standard on structures for transmissions. JEC-127-1979, Denkishoin, Japan. 1979.
60. John Holmes, et al. A forensic study of the Lubbock-Reese downdraft of 2002. Wind and structures. 2008; 11(2): 137-152.
61. J. Armitt, et al. Calculation of wind loadings on components of overhead lines. In Proceedings of the Institution of Electrical Engineers. 1975; 122(11): 1247-1252.
62. Haitham Aboshosha, and Ashraf El Damatty. Span reduction factor of transmission line conductors under downburst winds. J Wind Eng. 2014; 11(1): 13-22.
63. M. Chay, et al. Wind loads on transmission line structures in simulated downbursts. 2006.
64. John Holmes. Along-wind response of lattice towers: part I-derivation of expressions for gust

response factors. Engineering Structures. 1994; 16(4): 287-292.

65. G. Solari. Analytical estimation of the alongwind response of structures. Journal of Wind Engineering and Industrial Aerodynamics. 1983; 14(1-3): 467-477.
66. Claës Dyrbye, and Svend Hansen. Calculation of joint acceptance function for line-like structures. Journal of Wind Engineering and Industrial Aerodynamics. 1988; 31(2-3): 351-353.
67. Nicolas Blaise, et al. Calculation of third order joint acceptance function for line-like structures. In XIII Conference of the Italian Association for Wind Engineering. 2014.
68. Pham Hung, et al. Large amplitude vibrations of long-span transmission lines with bundled conductors in gusty wind. Journal of Wind Engineering and Industrial Aerodynamics. 2014; 126: 48-59.
69. Haiwei Xu, et al. Wind-induced swing investigation on transmission line jumper wire under hilly terrain. Journal of Zhejiang University. 2017; 51(2): 264-272.
70. Chuncheng Liu, et al. Study on wind-induced swing response characteristics of transmission lines under mountain terrain. Journal of Basic Science and Engineering. 2021; 29(4): 1044-1056.
71. Chuncheng Liu, and Hongyun Sun. Wind deflection characteristics of transmission lines under terrain conditions of canyon and pass. Journal of Vibration and Shock. 2021; 40(9): 184-194.
72. Wenjuan Lou, et al. Properties of mountainous terrain wind field and their influence on wind-induced swing of transmission lines. China Civil Engineering Journal. 2018; 51(10): 46-55.
73. Wenlong Du, et al. Time–Frequency Buffeting Responses of Transmission Lines Excited by Two-Dimensional Turbulent Wind: Closed-Form Solution. Journal of Engineering Mechanics. 2023; 149(12): 04023101.
74. Chao Zhou, et al. Effects of wind and rain on the motion of the high-voltage conductor in a simplified valley terrain. Electric Power Systems Research. 2019; 173: 153-163.
75. Yuelong Zhang, et al. Aerodynamic force characteristics and wind-induced swing analysis of ellipse iced conductor with ice bridge. Journal of South China University of Technology (Natural Science Edition). 2021; 49(7) :125-133.
76. Wenjuan Lou, et al. An improved rigid rod method for wind-induced swing response prediction of heavily iced transmission lines. Journal of Wind Engineering and Industrial Aerodynamics. 2023; 235: 105358.
77. Wenjuan Lou, et al. Fluctuating aerodynamic characteristics and wind-induced swing response of typical iced conductors. Journal of Zhejiang University (Engineering Science). 2017; 51(10): 1988-1995.
78. Shuguo Liang, et al. Analysis of three dimensional equivalent static wind loads of symmetric high-rise buildings based on wind tunnel tests. Wind and Structures. 2014; 19(5): 565-583.
79. Wenjuan Lou, et al. Multiobjective equivalent static wind loads on complex tall buildings using non-gaussian peak factors. Journal of Structural Engineering. 2015; 141(11): 04015033.

80. Wenjuan Lou, et al. Calculation method for equivalent static wind loads and wind load adjustment coefficients for transmission lines. Journal of Zhejiang University (Engineering Science). 2016; 50(11): 2120-2127.
81. Xin Hu, et al. Dynamic wind-induced deflection response characteristics of insulator string under slope wind attack angle. High Voltage Engineering. 2022; 48(1): 289-297.